

# Influence of grinding wheel velocity on the wear of electroplated cBN grinding wheel

Wpływ prędkości szlifowania na zużywanie się ściernicy z nasypem z cBN, ze spoiwem nanoszonym galwanicznie

ANDRZEJ KAWALEC  
ANNA BAZAN  
MAREK KROK\*

DOI: <https://doi.org/10.17814/mechanik.2017.8-9.101>

Presented are the results of research on changes of the grinding force components and selected topography parameters of grinding wheel active surface during grinding wheel life. Electroplated cBN grinding wheels working with different rotation speeds were examined.

**KEYWORDS:** grinding wheel wear, electroplated cBN grinding wheels

The speed of grinding  $v_s$  can affect the machining effects in different ways. Increase in  $v_s$  value increases the temperature in the grinding zone, leading to lower hardness of the material and its shear strength. There is also a reduction in the grain size in the workpiece, which, on the one hand, translates into lower grain loading, but on the other hand it adversely affects the effective rake angle and can lead to an increase in shear strength as a result of the shear strength of the chip.

In the case of monolayer wheels with cBN embankment, it is more often observed that the increase in grinding speed is accompanied by a decrease in the grinding force [2-6]. Except for the work [2], the publications do not discuss the changes occurring on the active surface of the grinding wheel (GWAS) due to wear at different grinding speeds.

The article presents the results of the research on changes of grinding force and CPS topography under the influence of active wear of grinding wheels with cobalt binders working at different rotational speeds.

## Methodology of research

Grinding of high alloy steel Pyrowear 53 was carried out on a Fortis sandblast by Michael Deckel, using a single-layer grinding wheel with a brazing platen, with a cBN abrasive and B35 grain size number. Wheels manufacturer (Shinhan Diamond) described the grains used as monocrystalline, semi-blocky (fig. 1).

The wheel has a conical shape with a maximum diameter of  $d_s = 100$  mm and a cone angle of  $140^\circ$ . The minimum hardness of the sanded layer was 81 HRA.

Three grinding wheels were used in the study, which worked with another set of adjustable parameters. In each of the three cases, the feed rate was  $v_w = 4250$  mm/min,

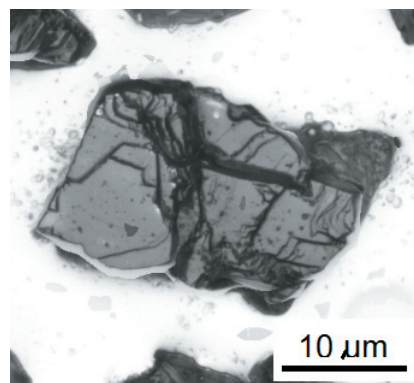


Fig. 1. Monocrystalline grain of semi-block cBN type on new grinding wheel

the grinding depth  $a_e = 20$   $\mu\text{m}$ , and the rotational speed  $n$  was changed to 4000, 6000 and 8000 rpm. Due to the available amount of workpiece, each grinding wheel could be removed with a wheel width (1 mm) to 2850 mm<sup>3</sup>.

During grinding, the grinding force components were measured using a Kistler 9123C rotary dynamometer, coupled to the 5223B amplifier and the NI USB-6009 measuring card. Signals were recorded in LabVIEW Signal Express 2012 with a sampling rate of 5 kS/s. For further processing of signals, including the determination of tangential ( $F_t$ ) and normal ( $F_n$ ) values, the Python programming environment was used.

The aim of the research was to assume that (GWAS) topography measurements would be conducted at different stages of wheel wear. Breaking the grinding process with a grinding wheel to measure its micro-geometry, however, proved to be too time consuming, so the (GWAS) topography was decided to be replicated with the replica.

Replicas were made using Struers' RepliSet system. The replica material was black silicone rubber, capable of reproducing details above 0.1  $\mu\text{m}$ . For the topography of (GWAS) replicas, the InfiniteFocus microscope from Alicona and the 20 $\times$  lens were used. After removing a given volume of material, six areas of 2.35  $\times$  2.59 mm on each wheel were measured. The vertical resolution was 0.1  $\mu\text{m}$ , the horizontal resolution was 5  $\mu\text{m}$ , the sampling rate was 0.44  $\times$  0.44  $\mu\text{m}$ . Analysis of measurement data with the determination of surface topography parameters was carried out in SPIP program 6.4.2.

InfiniteFocus microscope also used to perform all of the (GWAS) images shown in this article.

\* Dr hab. inż. Andrzej Kawalec (ak@prz.edu.pl), mgr inż. Anna Bazan (abazan@prz.edu.pl), mgr inż. Marek Krok (mkrok@prz.edu.pl) – Politechnika Rzeszowska

## Variation of grinding force components

The speed of grinding, which depends on the rotational speed of the grinding wheel, it had a very significant effect on the grinding wheel life and the value and the variation of the grinding force components (fig. 2). The higher grinding speed was related to lower values of the specific tangential force ( $F'_t$ ) and normal force ( $F'_n$ ) and longer wheel life.

For all three grinding wheels, a period of stable wear can be observed, which is approximately equal to the increase in the grinding force components together with the volume of material removed. In the study of grinding wheels at 4000 rpm and 6000 rpm, the wear intensity of the grinding wheel was also manifested by a very rapid increase in grinding force. In the case of the grinding wheel with the smallest grinding speed, the intensive wear phase started after the appropriate material loss of material  $V'$  of about  $58 \text{ mm}^3/\text{mm}$ . The stable speed of the grinding wheel at a rotational speed of  $n = 6000 \text{ rpm}$  ended at a material defect value of approximately  $V' = 680 \text{ mm}^3/\text{mm}$ . Wheels with a rotational speed of  $n = 8000 \text{ rpm}$  sanded the entire installed volume of material  $V' = 2850 \text{ mm}^3/\text{mm}$  without entering the intensive wear phase.

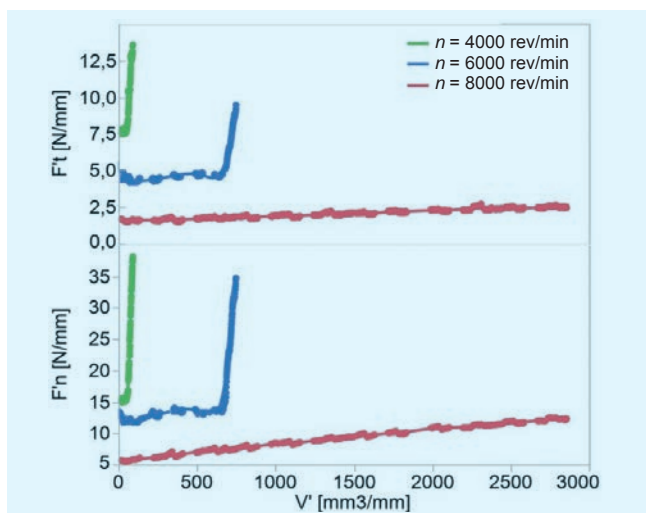


Fig. 2. The course of the value of the correct specific tangential grinding force ( $F'_t$ ) and the specific normal grinding force ( $F'_n$ ), depending on the correct material loss  $V'$

## Observed forms of CPS wear

Direct GWAS microscopic observation of all grinding wheels after the grinding process has allowed the following forms of wear to be recognized:

- crushing of grains (fig. 3) – the dominant form of wear of all tested grinding wheels. Due to the irregular shape of the new grains and too little magnification obtained with the aid of a microscope, it was not possible to observe macro-crumbs,
- grafting (fig. 4) – the form of grinding wear observed on all grinding wheels; the least occurring on a wheel with a rotational speed of 8000 rpm,
- grinding of grains (fig. 5) – relatively rare form of grain wear on the wheel with the highest rotational speed,
- GWAS sticking (fig. 6) – occurring on all examined wheels.

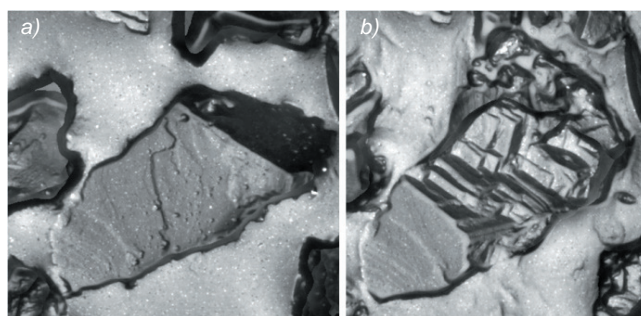


Fig. 3. Example of grain crushing: a) new grain, b) grain with macro-crumbs

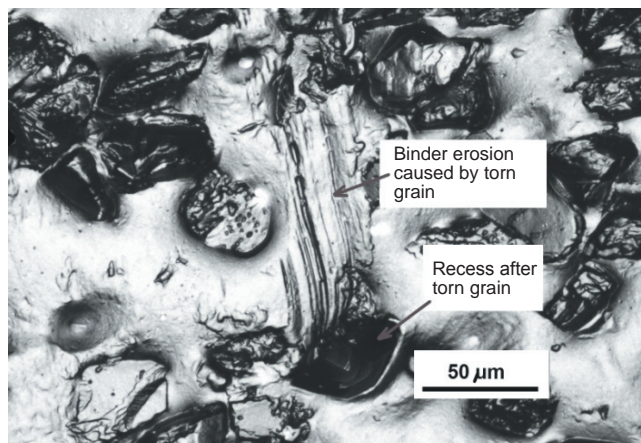


Fig. 4. Example of grain break

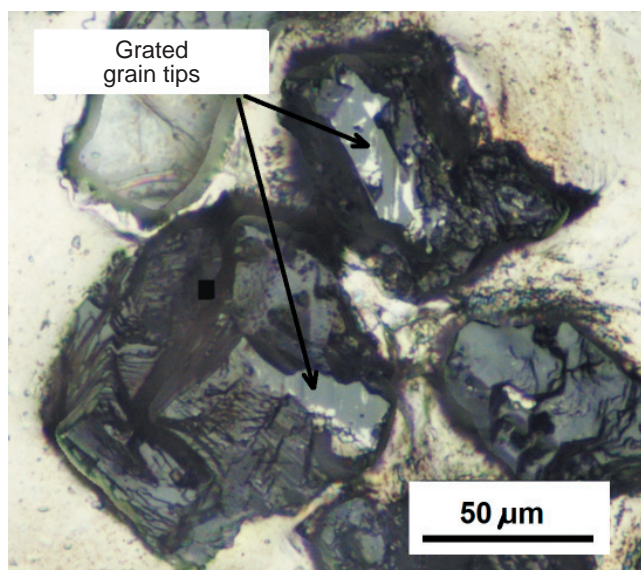


Fig. 5. Example of cBN grain grating

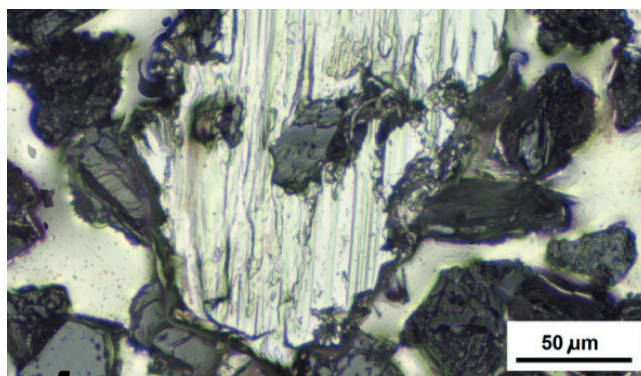


Fig. 6. Bonding on the active surface of the grinding wheel



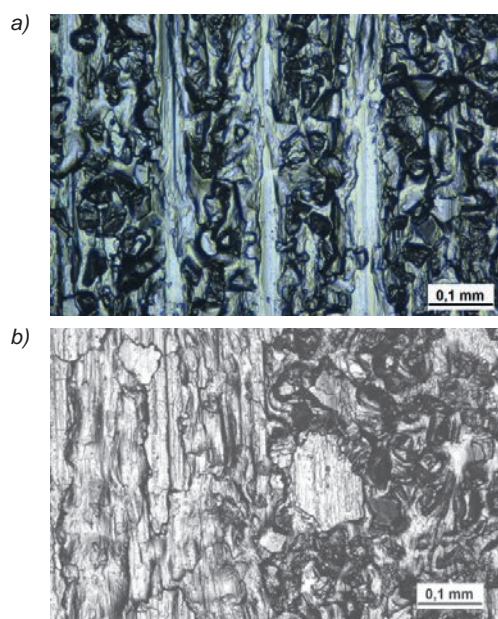


Fig. 7. Abrasion of the abrasive: a) initial phase with narrow belts of abraded abrasive, b) extensive abrasion loss (left)

### Change of GWAS topography parameters along with wear

For the analysis of GWAS topography, the parameters that have been reported in other studies on cobalt-grade cobalt-based grinding wheels show the highest classification capacity between new and used grinding wheels and the highest „sensitivity” to wear, i.e.  $Vmp$ ,  $Sbi$ ,  $Sci$  and  $Ssk$  [7]. Fig. 8 shows the course of the values of these parameters depending on the volume of the material removed. Each measuring point on the graph was created after averaging the determined value for the six surfaces on the specified wheel.

For all grinding wheels with the volume of material removed, the  $Vmp$ ,  $Sci$  and  $Ssk$  values are dropped. For grinding wheels operating at 6000 rpm and 8000 rpm, it is apparent that the intensity of the variation in the parameter values is higher in the initial test phase. For the grinding wheel at  $n = 4000$  rpm, this observation can not be verified due to the low number of GWAS tested due to its very rapid wear. However, it can be determined that the lower grinding speed is related to the greater intensity of the decrease in the values of the parameters in question.

The  $Vmp$  parameter indicates the volume of the highest elevations. The reduction may be due to high grafting, grating of grains or abrasion.

The liquid retention of the  $Sci$  core is related to the volume of voids in the core zone and the average square surface unevenness. This reduction is probably due to the occurrence of overstressing and, above all, the reduction in the height of the core zone caused by the crushing or grinding of the grain.

The value of the  $Ssk$  (surface asymmetry) parameter indicates the dominance of the elevations ( $Ssk > 0$ ) or the recesses ( $Ssk < 0$ ) on the surface. Reduction of this parameter suggests that abrasive abrasion predominates on the abrasive wheel.

$Sbi$  value increased with volume of material removed. This may be related to lowering of the highest eleva-

tions as well as to the general flattening of the topography, which results in a decrease in the  $Sq$  parameter. This in turn involves the wear of the grinding wheel and expresses in terms of height and volume parameters.

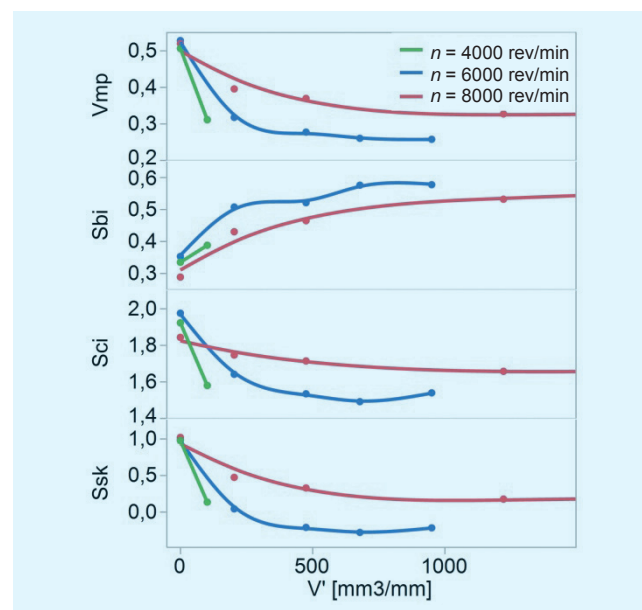


Fig. 8. Values of selected topography parameters of grinding wheel active surfaces at different rotational speeds  $n$  depending on the appropriate material loss  $V'$

### Conclusions

The rotational speed of the wheel during the test had a significant effect on the value of the grinding force components. Different grain loading conditions affected the intensity of wear.

GWAS wear is reflected in changes in surface topography that can be tracked using quantitative parameters. For any of the analyzed GWAS topography parameters, it was not possible to determine that grinding wheels enter the intensive wear phase after exceeding a certain limit value of this parameter.

### REFERENCES

1. Ghosh S., Paul S., Chattopadhyay A. "Experimental investigations on grindability of bearing steel under high efficiency deep grinding (HEDG)". *International Journal of Abrasive Technology*. 2, 2 (2009): s. 154-172.
2. Shi Z. "Grinding with electroplated cubic boron nitride (CBN) wheels". Praca doktorska. Amherst: University of Massachusetts, 2004.
3. Ding W. i in. "Grindability and surface integrity of cast nickel-based superalloy in creep feed grinding with brazed CBN abrasive wheels". *Journal of Aeronautics*. 23, 4 (2010): s. 501-510.
4. Pal A. i in. "Performance study of brazed type cBN grinding wheel on hardened bearing steel and high speed steel". *International Journal of Precision Engineering and Manufacturing*. 13, 5 (2012): s. 649-654.
5. Ichida Y. i in. "Formation mechanism of finished surface in ultrahigh-speed grinding with cubic boron nitride (cBN) wheels". *JSME International Journal Series C Mechanical Systems, Machine Elements and Manufacturing*. 49, 1 (2006): s. 100-105.
6. Burrows J. i in. "Grinding of Inconel 718 and Udimet 720 using superabrasive grinding points mounted on a high speed machining centre". *Proceedings of the 33rd International MATADOR Conference: Formerly The International Machine Tool Design and Research Conference* (2000).
7. Kawalec A., Bazan A., Krok M., Chmielik I. „Porównanie wyników badań stykowych dotyczących parametrów topografii CPS ściernic z CBN zmieniających się wraz z jej zużyciem". *XXXVIII Naukowa Szkoła Obróbki Ściernej. Mechanik*. 87, 8-9 (2015): CD s. 190-193. ■